



<http://www.diva-portal.org>

Postprint

This is the accepted version of a paper published in *Journal of the American Chemical Society*. This paper has been peer-reviewed but does not include the final publisher proof-corrections or journal pagination.

Citation for the original published paper (version of record):

Andersson, C., Öhrström, M., Popović-Bijelić, A., Gräslund, A., Stenmark, P. et al. (2012)
The manganese ion of the heterodinuclear Mn/Fe cofactor in *Chlamydia trachomatis*
ribonucleotide reductase R2c is located at metal position 1..
Journal of the American Chemical Society, 134(1): 123-125
<http://dx.doi.org/10.1021/ja209678x>

Access to the published version may require subscription.

N.B. When citing this work, cite the original published paper.

Permanent link to this version:

<http://urn.kb.se/resolve?urn=urn:nbn:se:su:diva-75648>

The Manganese Ion of the Heterodinuclear Mn/Fe Cofactor in *Chlamydia trachomatis* Ribonucleotide Reductase R2c is located at metal position 1

Charlotta S. Andersson, Maria Öhrström, Ana Popović-Bijelić[†], Astrid Gräslund, Pål Stenmark and Martin Högbom*

Department of Biochemistry and Biophysics, Stockholm University, S-10691 Stockholm, Sweden

Supporting Information Placeholder

ABSTRACT: The essential catalytic radical of Class-I ribonucleotide reductase is generated and delivered by protein R2, carrying a dinuclear metal cofactor. A new R2 subclass, R2c, prototyped by the *Chlamydia trachomatis* protein was recently discovered. This protein carries an oxygen-activating heterodinuclear Mn(II)/Fe(II) metal cofactor and generates a radical-equivalent Mn(IV)/Fe(III) oxidation state of the metal site, as opposed to the tyrosyl radical generated by other R2 subclasses. The metal arrangement of the heterodinuclear cofactor remains unknown. Is the metal positioning specific, and if so, where is which ion located? Here we use X-ray crystallography with anomalous scattering to show that the metal arrangement of this cofactor is specific with the manganese ion occupying metal position 1. This is the position proximal to the tyrosyl radical site in other R2 proteins and consistent with the assumption that the high-valent Mn(IV) species functions as a direct substitute for the tyrosyl radical.

Ribonucleotide reductase (RNR) performs the reduction of all four ribonucleotides to their corresponding deoxyribonucleotide via a radical mechanism. The radical generating R2 protein of Class-I RNR uses a di-metal carboxylate cofactor to produce, store and reversibly deliver the essential radical to the catalytic R1 subunit.¹⁻³ Class Ic R2 proteins (R2c), prototyped by the *Chlamydia trachomatis* R2c (CtR2c), is a recently discovered group that utilize a heterodinuclear Mn/Fe cofactor. Upon reaction with molecular oxygen, the reduced Mn(II)/Fe(II) site in CtR2c generates a Mn(IV)/Fe(III) radical equivalent oxidation state that is used in place of the standard tyrosyl radical, used by subclasses Ia and Ib.⁴⁻⁷ Class Ic R2 proteins carry a Phe residue in the position where the radical-harboring Tyr is found in subclasses Ia and Ib (Figure 1).^{5,8} R2c sequences are found in several bacteria and archaea, in particular among extremophiles and pathogens.⁸ Despite extensive biochemical, spectroscopic and computational studies, the arrangement of the heterodinuclear cofactor remains unknown. It is thus unclear if the positioning of the metals is specific, and if so, at which position they are located.

Here we use X-ray crystallography with anomalous scattering to show that the manganese ion in CtR2c is specifically located in

position 1 of the metal site. This position is the one neighboring the otherwise radical-harboring tyrosine in Class-Ia and -Ib R2 proteins and connected to the proposed radical transfer path between proteins R2 and R1.

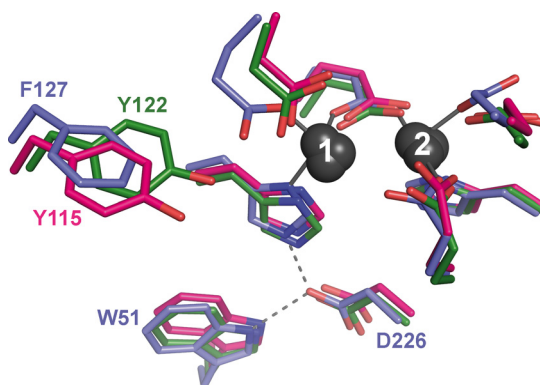


Figure 1. Superposition of R2 protein metal sites: Class Ia (green, *Escherichia coli*, PDB id 1MXR¹⁵), Class Ib (red, *Corynebacterium ammoniagenes*, PDB id 3MJO¹⁶) and Class Ic (blue, *Chlamydia trachomatis*, PDB id 1SY5⁵). Metal positions are indicated as well as the radical harboring tyrosine residues of subclasses Ia and Ib (Y122, Y115), in subclass Ic this position is occupied by a Phe (F127). Part of the hydrogen-bonded chain of conserved residues, proposed to be involved in radical transfer between proteins R2 and R1 is also indicated (D226, W51, *C. trachomatis* numbering).

Production of CtR2c by *E. coli* overexpression in standard rich medium yields a very low Mn content with accompanying low activity.^{7,9} To obtain high activity the protein either has to be produced in Mn-supplemented media or by preparation of metal depleted protein followed by metal reconstitution while minimizing the formation of a stable homodinuclear diiron site.^{7,10} Depending on the method of preparation, a fraction of the sample always contains the diiron site, which forms in parallel with the highly active heterodinuclear Mn/Fe cofactor.^{5,7,10-12} For this study the protein was produced by overexpression in *E. coli* grown in Mn-supplemented rich medium, as previously described.^{9,12} Metal content of the CtR2c protein and ribonucleotide reductase activity with *C. trachomatis* R1 was confirmed to be at par with previously published data for this method of preparation. The numbers differed slightly between batches with a specific activity between 100

and $150 \text{ nmol min}^{-1} \text{ mg}^{-1}$ and a metal content of 1-1.45 equivalents of Fe and 0.35-0.45 equivalents of Mn per polypeptide. Higher manganese content corresponded to higher activity, as also previously observed.^{7,9-12} Crystallization of the protein as described previously¹³ yielded crystals diffracting to high resolution (1.5 \AA , Supporting table 1). Anomalous dispersion measurements revealed that an anomalous scatterer, most likely Pb(II) from the crystallization solution, was present in the dinuclear site. The strong Pb anomalous signal precluded a direct and unambiguous observation of a manganese anomalous signal. For a detailed description and analysis of this data see Supporting Material.

To be able to directly observe the anomalous signal from both Mn and Fe, and thus the complete heterodinuclear cofactor in the protein, a crystallization condition not including lead was identified ($3 \mu\text{l}$ of protein at 3 mg/ml in 12 mM Tris-HCl buffer at pH 7.5, 1 mM MnCl_2 , 1 mM MgCl_2 was mixed with $0.5 \mu\text{l}$ 0.1 M MES pH 6.2, 9% PEG 20K and left to equilibrate over the same solution). This condition produced crystals diffracting to lower resolution, 3.2 \AA , but still sufficient to measure the Mn and Fe anomalous signals in the absence of any disturbing anomalous scatterers. Anomalous dispersion data were collected at $\lambda = 1.7 \text{ \AA}$ (high energy side of Fe K-edge) 1.85 \AA (Between Mn and Fe K-edges) and 1.92 \AA (low energy side of Mn K-edge)(Supporting Figure 1). At $\lambda = 1.85 \text{ \AA}$ Mn, but not Fe, displays an anomalous signal. As shown in Figure 2(a) Mn is exclusively located in position 1 of the metal site with no signal above noise level in position 2. At $\lambda = 1.7 \text{ \AA}$ both Mn and Fe, display anomalous signals. As shown in Figure 2(b) an anomalous signal, not present at $\lambda = 1.85 \text{ \AA}$ appears in position 2 of the metal site showing the presence of iron in this position. The data collected at $\lambda = 1.92 \text{ \AA}$ showed no anomalous signal above noise level in the dinuclear site, confirming that Mn and Fe are the only contributors to the signals observed at $\lambda = 1.85 \text{ \AA}$ and 1.7 \AA . From this data it is not possible to define if a low occupancy of iron is present in site 1, which would indicate that a fraction of the sample contained a diiron site, as generally observed.^{5,7,10-12} The existence of a diiron site at partial occupancy is however directly observed in the data from the Pb-containing crystal, showing that site 2 is virtually fully occupied by Fe and that site 1 contains a smaller, but detectable, amount of iron (Supporting Material). The limited resolution of the lead-free crystals prohibits a detailed analysis of the metal coordination or redox-dependent structural changes of the heterodinuclear cofactor. Work to obtain high-resolution structures of the fully occupied site for such studies is ongoing.

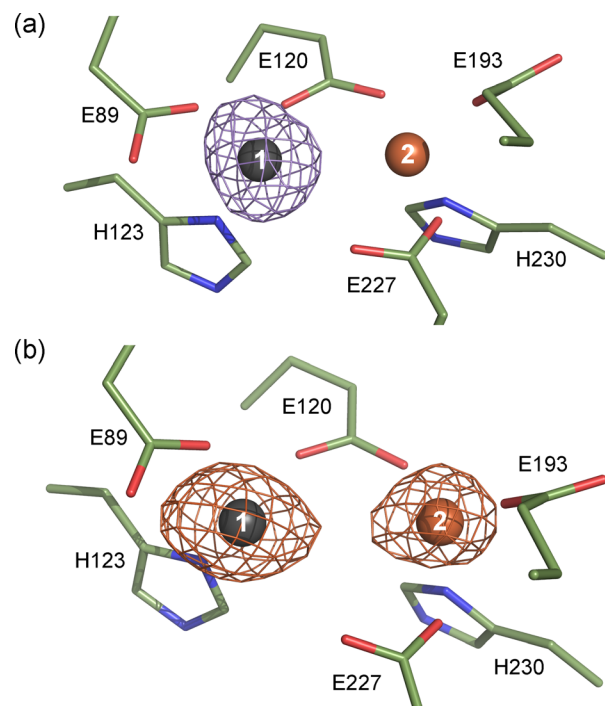


Figure 2. (a) Anomalous difference map at $\lambda = 1.85 \text{ \AA}$ where Mn, but not Fe, display anomalous scattering, contoured at 0.08 e\AA^{-3} . (b) Anomalous difference map at $\lambda = 1.7 \text{ \AA}$ where both Mn and Fe display anomalous scattering, contoured at 0.08 e\AA^{-3} . The data show that Mn is located in metal position 1 but not metal position 2. The appearance of an anomalous signal in position 2 at $\lambda = 1.7 \text{ \AA}$ shows that Fe is located in this position. The absence of any anomalous scatterers other than Fe and Mn was verified by a dataset collected at $\lambda = 1.92 \text{ \AA}$.

Together, these data show that production of the protein, also in Mn-enriched media, results in Fe exclusively occupying metal position 2. Moreover, Fe-binding in position 2 is not displaced either by incubation of the protein with 1 mM Mn(II) or 0.33 mM Pb(II) and thus likely of high affinity. Position 1, on the other hand, can accommodate Mn, Fe as well as Pb. The arrangement with Mn in site 1 and Fe in site 2 of the active cofactor is the same arrangement as observed in the recently discovered R2lox protein from *Mycobacterium tuberculosis*, which also possesses a heterodinuclear Mn/Fe cofactor.¹⁴ From a functional perspective, it is interesting to note that the high-valent Mn(IV) ion is located in the position proximal to the radical harboring tyrosine in subclasses Ia and Ib. The metal ion in this position is directly coordinated by a residue from the hydrogen-bonded chain of conserved residues, proposed to take part in the radical transfer between proteins R2 and R1.¹ Positioning the radical-initiating species in this site could suggest that only minimal additional adaptations are required in the radical transfer mechanism compared to the tyrosyl radical containing RNRs.

ASSOCIATED CONTENT

Supporting Information. Supporting results, figures, experimental procedures, and crystallographic statistics are included as Supporting Information. This material is available free of charge via the Internet at <http://pubs.acs.org>.

AUTHOR INFORMATION

Corresponding Author

* hogbom@dbb.su.se

Present Addresses

†University of Belgrade, faculty of physical chemistry.

Funding Sources

This work was supported by the Swedish research council (2010-5061, 2010-5200, 2010-4950) to MH, PS and AG, the Wenner-Gren foundations and the Swedish foundation for strategic research to MH and PS.

ACKNOWLEDGMENT

We are grateful to the staff at beamline MX 14.1 at HZB, BESSY II for support with long-wavelength data collection.

ABBREVIATIONS

CtR2c, *Chlamydia trachomatis* protein R2.

REFERENCES

- (1) Nordlund, P.; Reichard, P. *Annu. Rev. Biochem.* **2006**, *75*, 681-706.
- (2) Högbom, M. *Metallomics* **2011**, *3*, 110-120.
- (3) Cotruvo, J. A.; Stubbe, J. *Annu. Rev. Biochem.* **2011**, *80*, 733-767.
- (4) Roshick, C.; Iliffe-Lee, E. R.; McClarty, G. J. *Biol. Chem.* **2000**, *275*, 38111-38119.
- (5) Högbom, M.; Stenmark, P.; Voevodskaya, N.; McClarty, G.; Gräslund, A.; Nordlund, P. *Science* **2004**, *305*, 245-248.
- (6) Jiang, W.; Yun, D.; Saleh, L.; Bollinger, J. M., Jr.; Krebs, C. *Biochemistry* **2008**, *47*, 13736-13744.
- (7) Jiang, W.; Yun, D.; Saleh, L.; Barr, E. W.; Xing, G.; Hoffart, L. M.; Maslak, M. A.; Krebs, C.; Bollinger, J. M., Jr. *Science* **2007**, *316*, 1188-1191.
- (8) Högbom, M. *J Biol Inorg Chem* **2010**, *15*, 339-349.
- (9) Popovic-Bijelic, A.; Voevodskaya, N.; Domkin, V.; Thelander, L.; Gräslund, A. *Biochemistry* **2009**, *48*, 6532-6539.
- (10) Jiang, W.; Hoffart, L. M.; Krebs, C.; Bollinger, J. M., Jr. *Biochemistry* **2007**, *46*, 8709-8716.
- (11) Jiang, W.; Bollinger, J. M., Jr.; Krebs, C. *J. Am. Chem. Soc.* **2007**, *129*, 7504-7505.
- (12) Voevodskaya, N.; Lenzian, F.; Sanganas, O.; Grundmeier, A.; Gräslund, A.; Haumann, M. *J. Biol. Chem.* **2009**, *284*, 4555-4566.
- (13) Stenmark, P.; Hogbom, M.; Roshick, C.; McClarty, G.; Nordlund, P. *Acta. Cryst. D-Biol. Cryst.* **2004**, *60*, 376-378.
- (14) Andersson, C. S.; Högbom, M. *Proc. Natl. Acad. Sci. USA* **2009**, *106*, 5633-5638.
- (15) Högbom, M.; Galander, M.; Andersson, M.; Kolberg, M.; Hofbauer, W.; Lassmann, G.; Nordlund, P.; Lenzian, F. *Proc. Natl. Acad. Sci. USA* **2003**, *100*, 3209-3214.
- (16) Cox, N.; Ogata, H.; Stolle, P.; Reijerse, E.; Auling, G.; Lubitz, W. *J. Am. Chem. Soc.* **2010**, *132*, 11197-11213.

Supporting Material

The Manganese Ion of the Heterodinuclear Mn/Fe Cofactor in *Chlamydia trachomatis* Ribonucleotide Reductase R2c is located at metal position 1

Charlotta S. Andersson, Maria Öhrström, Ana Popović-Bijelić, Astrid Gräslund, Pål Stenmark and Martin Högbom*

Department of Biochemistry and Biophysics, Stockholm University, S-10691 Stockholm, Sweden

Contents:

1. Supporting results
2. Experimental procedures
3. Supporting Tables 1-2
4. Supporting Figures 1-3
5. References

1. Supporting Results

Crystals prepared in the presence of Pb(II). The as-prepared protein was crystallized as described previously, in particular the presence of 0.33 mM Pb(II) in the crystallization condition is needed to obtain crystals diffracting to high-resolution.¹ Crystals diffracting to 1.5 Å resolution was obtained and analyzed for anomalous scatterers through collecting data at $\lambda = 1.7$ Å (high energy side of Fe K-edge) $\lambda = 1.85$ Å (between Mn and Fe K-edges) and $\lambda = 1.92$ Å (low energy side of Mn K-edge) (Supporting figure 1). At $\lambda = 1.92$ Å, where neither Mn, nor Fe display an anomalous signal, a large anomalous peak was observed in metal position 1 (Supporting figure 2(a)). This indicated the presence of another strong scatterer. Most likely, Pb(II) from the crystallization solution binding at metal position 1, though far from any edge, Pb has a large anomalous signal at these wavelengths (Supporting figure 1). At $\lambda = 1.85$ Å where both Pb and Mn display anomalous signals, a similar peak was observed in position 1 (Supporting figure 2(b)), notably no anomalous signal above the map noise level was observed in metal position 2 showing that neither Mn nor Pb was present in position 2 of the metal site. At $\lambda = 1.7$ Å, where Pb, Mn and Fe display anomalous signals, an anomalous peak appeared also in metal position 2 (Supporting figure 2(c)), showing the presence of Fe in this site. The anomalous signal at $\lambda = 1.7$ Å in position 2 is notably weaker than in position 1, as would be expected because Pb is a stronger anomalous scatterer at this wavelength (Supporting figure 1).

The well-diffracting crystal in this case allowed low-dose collection of anomalous data to minimize radiation damage for calculation of double-difference (ddano) anomalous maps as described previously.² It should be noted that these types of subtractions are heavily dependent on the relative scaling of the datasets and, even with carefully collected data, the results are mainly qualitatively meaningful. A Mn-specific ddano map (in principle subtracting the anomalous signal at $\lambda = 1.92$ Å from that at $\lambda = 1.85$ Å, for a detailed description of the procedure see Than *et al.*)²

showed only a noise-level peak in position 1. The presence of Mn could thus not be unambiguously assigned from this data.

A $d_{ano_{1.7\text{\AA}}}-d_{ano_{1.92\text{\AA}}}$ double-difference (ddano) map, in essence removing the Pb anomalous signal (Supporting figure 3(a)) shows a smaller, but significant, peak also in site 1, indicating the presence of Fe or Mn, in addition to Pb, in position 1. A $d_{ano_{1.7\text{\AA}}}-d_{ano_{1.85\text{\AA}}}$ ddano map (removing the contributions from both Pb and Mn) also shows some remaining anomalous signal in position 1 (Supporting figure 3(b)). This indicates that Fe is also located in position 1 at low occupancy. It thus appears that a fraction of the sample contains a homodinuclear diiron site, as commonly observed using any method for preparation of this protein. The signal in position 1 of the $d_{ano_{1.7\text{\AA}}}-d_{ano_{1.85\text{\AA}}}$ ddano map is approaching the noise level and appears weaker (compared to the signal in position 2) than the signal observed in position 1 of the $d_{ano_{1.7\text{\AA}}}-d_{ano_{1.92\text{\AA}}}$ ddano map. Still, as noted above, ddano maps are not well suited for quantitative analysis and this cannot be taken as definitive proof of the presence of manganese in this position.

To roughly estimate the amount of the different metals in the dinuclear site in the crystal we used the high-resolution data from the same crystal (1.5 Å-resolution collected at $\lambda = 0.918$ Å) for occupancy refinement of the metal positions. Because occupancy is strongly correlated with B-factors, the B-factors for the metals were estimated to the average B of all protein atoms. The anomalous scattering analysis showed that only Fe is present in position 2. Occupancy refinement of this ion against the high-resolution data suggested that position 2 is essentially fully occupied by Fe ($0.8 \leq Q \leq 1.0$). The situation for position 1 is more complicated because it contains a mixture of metals. To be able to obtain an estimate of the relative presence of Pb and the lighter metals (Mn and Fe cannot be distinguished based on this type of analysis) we made the additional assumption that position 1 is fully occupied, so that $Q_{Pb}=1-Q_{(Fe+Mn)}$. Using these assumptions, occupancy refinement indicated that position 1 contains Pb and one or both of the lighter metals in roughly equal molar amounts ($0.35 \leq Q_{Pb} \leq 0.50$).

Together, this data shows that position 2 exclusively contains Fe and is practically fully occupied, with no trace of either Mn or Pb. Position 1, on the other hand, is occupied by Pb, Fe and, possibly, Mn. Given the metal content of this particular protein sample before crystallization, 1.45 equivalents Fe and 0.45 equivalents of Mn per R2c monomer, it appears likely that either Pb(II) has displaced Mn and/or Fe from position 1 in the dinuclear site, or a selection process is in effect during crystallization.

2. Experimental procedures

Protein Sample Preparation

Original plasmids and protocols for expression and purification of *C. trachomatis* R2c were obtained as a kind gift from Grant McClarty.³ To obtain Mn-Fe R2 protein, recombinant protein was expressed in *E.coli* BL21(DE3) in standard LB medium supplemented gradually with MnCl₂ up to a concentration of 100 μM as described previously.⁴ Purification was performed as previously described by ammonium sulfate precipitation and ion exchange chromatography. Protein samples were further purified by size-exclusion (Superdex75 10/300 GL, GE Healthcare) chromatography, in 12mM Tris-HCl, pH 7.5. The purified protein was concentrated to 4 mg ml⁻¹, in a Vivaspin centrifugal concentrator (Vivaproducts) with a molecular weight cut-off of 10 kDa.

Metal Content Determination and Activity Measurement

Manganese content was determined in an acid-denaturing procedure using EPR spectroscopy at 293 K with a 3mW microwave power and a modulation amplitude of 1mT. The concentration of manganese is determined by the amplitude of the EPR signal and is compared to a standard solution of 0.5mM MnCl₂.⁴ Iron content was spectrophotometrically determined using an iron/TIBC reagent set (Eagle Diagnostics). Slight variations of metal content were observed between protein batches. Samples used in this study typically contained 0.35-0.45 equivalents of

manganese, and 1.0-1.45 equivalents of iron per R2c polypeptide. Activity was verified by measuring reduction of [³H]CDP to dCDP, as described previously.⁵ The specific activity was in the range of 100 to 150 $\mu\text{mol min}^{-1} \text{mg}^{-1}$. Both metal content and specific activity was in accordance with previously reported results for this method of protein preparation.⁵

Crystallization, Data Collection and Processing

CtR2c protein was crystallized using the sitting drop vapour diffusion method, employing a heavy atom co-crystallization approach.¹ Optimal conditions were obtained from mixing 3 μl of protein solution at 3 mg ml^{-1} containing 0.33 mM $\text{Pb}(\text{CH}_3\text{COO})_2$ and 8 mM Tris-HCl pH 7.5 with 0.5 μl well solution consisting of 0.1 M MES pH 6.3, 3% PEG 20K. The crystal was soaked for a couple of minutes in mother liquor supplemented with 35% PEG400, before being flash-frozen in liquid nitrogen. Diffraction data were collected at 100° K at beamline MX_14.1 at the synchrotron radiation source BESSYII, operated by Helmholtz Zentrum Berlin (HZB) in Berlin, Germany. To determine metal identity in the two binding sites, anomalous data were collected on the high-energy sides of the manganese *K*-edge ($\lambda=1.85 \text{ \AA}$) and for the high-energy side of the *K*-edge for iron ($\lambda=1.7 \text{ \AA}$). An additional dataset was collected at an energy lower than the absorption edge for manganese ($\lambda=1.92 \text{ \AA}$), as a control for Pb scattering. Data was processed and scaled in iMOSFLM⁶ and SCALA.⁷ A high-resolution dataset was collected at $\lambda=0.92 \text{ \AA}$ and processed using *xds*.⁸ Data collection statistics are presented in **Table S1**. Phases were obtained from molecular replacement using the original *CtR2c* structure, PDB ID 1SYU.⁹ Anomalous-difference model-phased Fourier (DANO) maps were calculated using FFT.⁷ Anomalous double-difference maps were calculated according to Than *et al.*²

To avoid the presence of any disturbing anomalous scatterers, a new crystallization condition was identified. For this crystallization condition, pre-incubation of the *CtR2* protein with 1mM magnesium and 1 mM manganese was required to obtain crystals. The best crystals

were obtained in the following condition: 3 μl protein solution at 3 mg ml^{-1} in 8 mM Tris-HCl, pH 7.5, 1 mM MgCl_2 and 1 mM MnCl_2 was mixed with 0,5 μl reservoir solution 0.1 M MES, pH 6.0-6.4, 5-9% PEG 20K. The drops were streak-seeded a few minutes after setup to induce nucleation. Crystals grew from heavily precipitated drops within 4 days. The crystals were then briefly moved to a cryo protecting solution, constituted from mother liquor supplemented with 35% PEG400, before storage in liquid-nitrogen. Data collection was performed in the same manner as for the lead-incubated sample, with the only difference of data being processed with *xds*.⁸ Crystallographic data statistics are shown in **Table S2**.

3. Supporting Tables:

Table S1. Data statistics for the protein crystallized in the presence of lead.

	R2c_Pb $\lambda = 1.92\text{\AA}$	R2c_Mn $\lambda = 1.85\text{\AA}$	R2c_Fe $\lambda = 1.70\text{\AA}$	R2c $\lambda=0.92\text{\AA}$
Data Processing	mosflm	mosflm	mosflm	xds
Beamline	MX_14.1	MX_14.1	MX_14.1	MX_14.1
Wavelength, \AA	1.92	1.85	1.70	0.92
Space group	P4 ₃ 2 ₁ 2	P4 ₃ 2 ₁ 2	P4 ₃ 2 ₁ 2	P4 ₃ 2 ₁ 2
Cell parameters, \AA	62.8, 62.8, 172.3	62.9, 62.9, 172.3	62.8, 62.8, 172.3	62.8, 62.8, 172.2
Resolution, \AA	39-2.4 (2.51-2.38)	39-2.4 (2.51-2.38)	42-2.4 (2.50-2.38)	35-1.5 (1.59-1.50)
Completeness, %	99.8 (99.5)	99.8 (99.5)	99.9 (99.9)	99.6 (98.7)
Redundancy	4.9 (4.7)	4.9 (4.7)	5.0 (4.8)	6.3 (6.3)
Rsym, %	8.6 (30.3)	12.6 (46.6)	4.8 (10.1)	8.3 (61.8)
I/ σ I	7.2 (2.4)	5.4 (1.6)	11.0 (6.8)	14.6 (2.8)
RCR_anom ^{RCR}	1.4 (1.0)	1.2 (1.0)	1.6 (1.2)	-

RCR. The RMS Correlation Ratio, calculated from a scatter plot of pairs of DeltaI(anom).⁷

Table S2. Data statistics for the protein crystallized in the lead-free condition.

	R2c_Pb $\lambda = 1.92\text{\AA}$	R2c_Mn $\lambda = 1.85\text{\AA}$	R2c_Fe $\lambda = 1.70\text{\AA}$
Data Processing	xds	xds	xds
Beamline	MX_14.1	MX_14.1	MX_14.1
Wavelength, \AA	1.92	1.85	1.70
Space group	P4 ₃ 2 ₁ 2	P4 ₃ 2 ₁ 2	P4 ₃ 2 ₁ 2
Cell parameters, \AA	62.8, 62.8, 172.3	62.6, 62.6, 171.2	62.8, 62.8, 171.9
Resolution, \AA	35 - 3.7 (3.8-3.7)	35 - 3.2 (3.28-3.20)	35 - 3.2 (3.28-3.20)
Completeness, %	78.2 (74.9)	92.7 (81.5)	89.2 (76.6)
Redundancy	2.5 (1.9)	4.7 (4.1)	3.3 (2.8)
Rsym, %	17.0 (52.1)	13.6 (61.2)	10.4 (53.6)
I/ σ I	5.3 (1.5)	11.9 (2.3)	12.3 (2.1)
SigAno ^{SA}	1.0 (0.8)	1.0 (0.7)	1.0 (0.7)

SA. Mean anomalous difference in units of its estimated standard deviation ($|F(+)-F(-)|/\text{Sigma}$).⁸

4. Supporting Figures:

Figure S1. Anomalous scattering terms f' and f'' plotted as a function of X-ray energy and wavelength. The real anomalous coefficient f' indicates the K -edge i.e. the theoretical values for absorption and the imaginary scattering coefficient f'' . Plotted graphs for the three metals are indicated as following; lead (solid), manganese (dashed), and iron (dotted). Arrows indicate wavelengths used and their energetic location. Theoretical values were generated using the website: http://skuld.bmsc.washington.edu/scatter/AS_form.html.

Figure S2. *CtR2c* active site of protein crystallized in the presence of Pb(II). Anomalous difference maps were generated for data collected at specified wavelengths. (a) Anomalous difference map at $\lambda = 1.92 \text{ \AA}$, where neither Mn nor Fe display anomalous scattering, contoured at 0.09 e\AA^{-3} . (b) Anomalous difference map at $\lambda = 1.85 \text{ \AA}$, where Pb and Mn but not Fe display anomalous scattering, contoured at 0.10 e\AA^{-3} . (c) Anomalous difference map at $\lambda = 1.7 \text{ \AA}$, where Pb, Mn and Fe display anomalous scattering, contoured at 0.08 e\AA^{-3} .

Figure S3. Double-difference (ddano) maps of protein crystallized in the presence of Pb(II) to assess specific metal contributions to the anomalous signal. (a) $\text{dano}_{1.7\text{\AA}} - \text{dano}_{1.92\text{\AA}}$ map, removing the contributions from anomalous scatterers other than Mn and Fe, contoured at 0.09 e\AA^{-3} . (b) $\text{dano}_{1.7\text{\AA}} - \text{dano}_{1.85\text{\AA}}$ map; removing the contributions from anomalous scatterers other than Fe, contoured at 0.06 e\AA^{-3} .

Figure S1

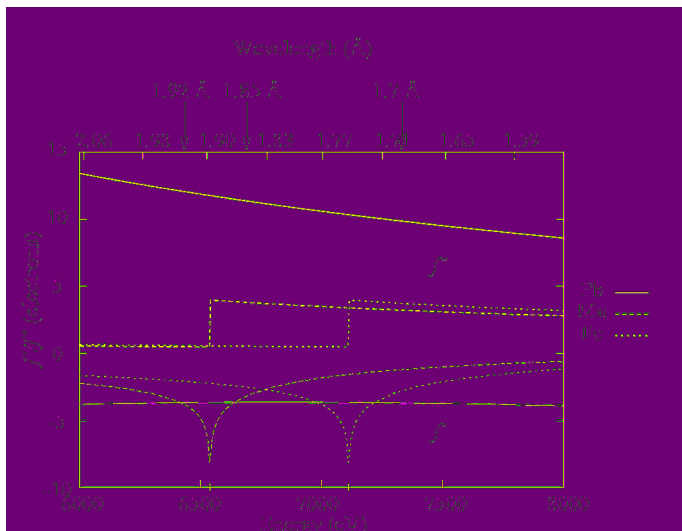


Figure S2

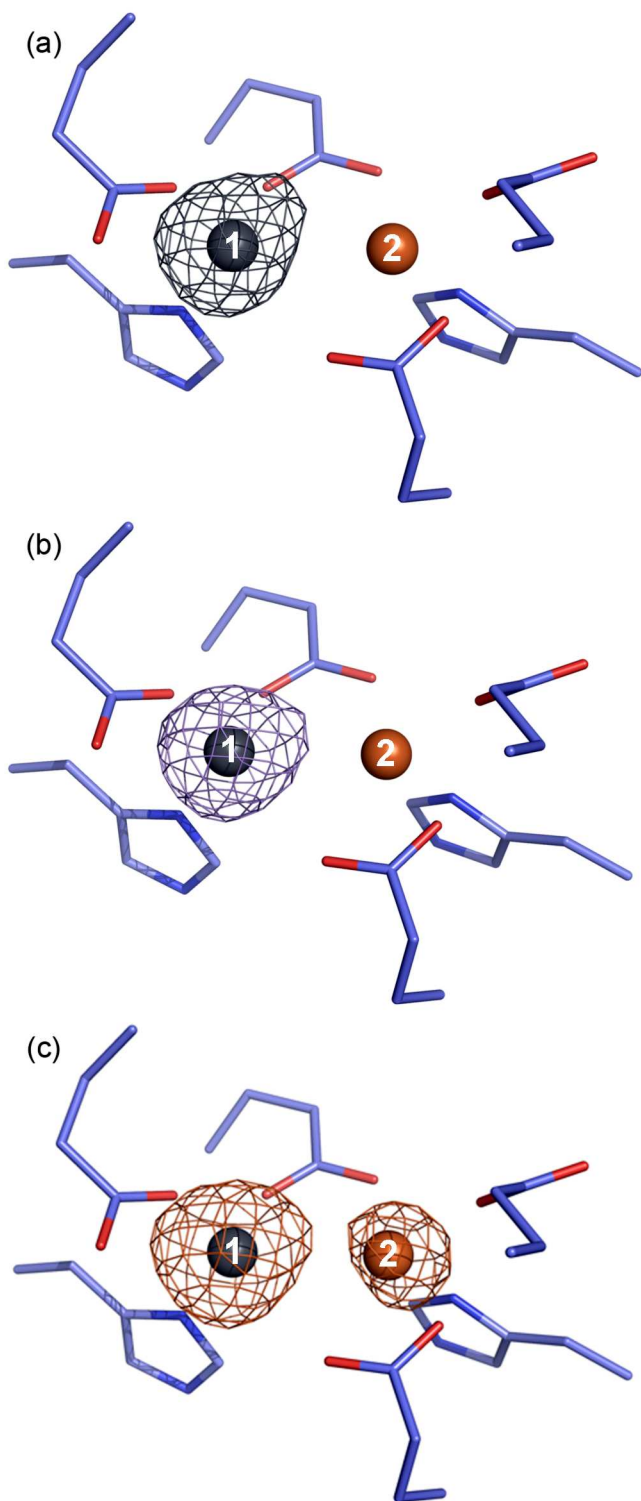
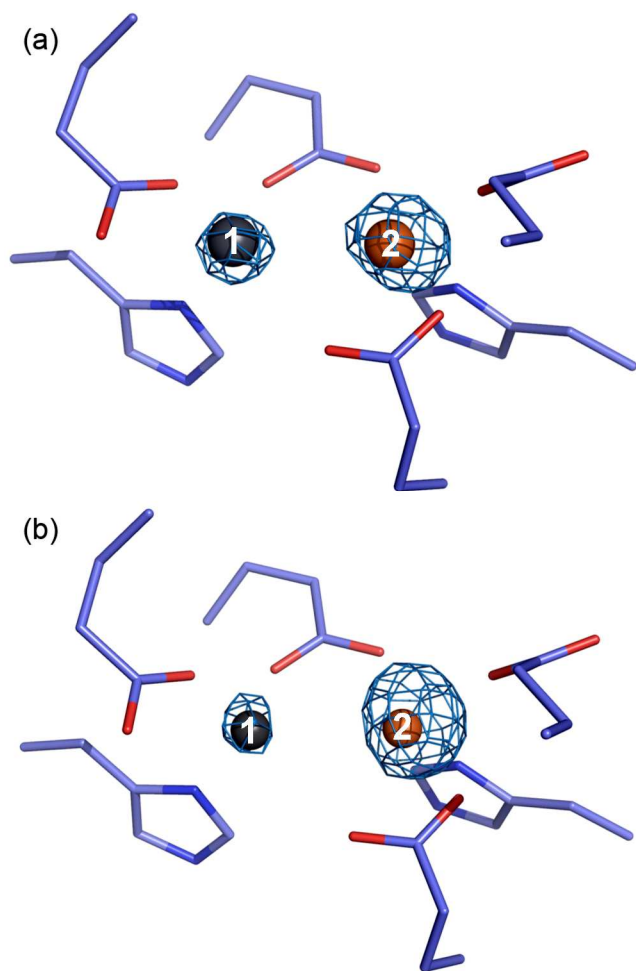


Figure S3



5. References

- (1) Stenmark, P.; Högbom, M.; Roshick, C.; McClarty, G.; Nordlund, P. *Acta Cryst. D Biol. Cryst.* **2004**, *60*, 376-8.
- (2) Than, M. E.; Henrich, S.; Bourenkov, G. P.; Bartunik, H. D.; Huber, R.; Bode, W. *Acta Cryst. D Biol. Cryst.* **2005**, *61*, 505-12.
- (3) Roshick, C.; Iliffe-Lee, E. R.; McClarty, G. *J. Biol. Chem.* **2000**, *275*, 38111-9.
- (4) Voevodskaya, N.; Lenzian, F.; Sanganas, O.; Grundmeier, A.; Gräslund, A.; Haumann, M. *J. Biol. Chem.* **2009**, *284*, 4555-66.
- (5) Popovic-Bijelic, A.; Voevodskaya, N.; Domkin, V.; Thelander, L.; Gräslund, A. *Biochemistry* **2009**, *48*, 6532-9.
- (6) Batty, T. G.; Kontogiannis, L.; Johnson, O.; Powell, H. R.; Leslie, A. G. *Acta Cryst. D Biol. Cryst.*, *67*, 271-81.
- (7) Collaborative computational project (1994) *Acta Cryst. C.* *50*:760–763
- (8) Kabsch, W. *Acta Cryst. D Biol. Cryst.*, *66*, 125-32.
- (9) Högbom, M.; Stenmark, P.; Voevodskaya, N.; McClarty, G.; Gräslund, A.; Nordlund, P. *Science* **2004**, *305*, 245-8.